JOURNAL OF Applied Polymer SCIENCE

Effect of graphene loading on thermomechanical properties of poly(vinyl alcohol)/starch blend

Jobin Jose,[1,2] Mamdouh A. Al-Harthi,[1,3] Mariam Al-Ali AlMa'adeed,[4] Jolly Bhadra Dakua,[4] Sadhan K. De[1]

[1]Department of Chemical Engineering, King Fahd University of Petroleum & Minerals, Dhahran 31261, Saudi Arabia
[2]Center for Engineering Research (CER), King Fahd University of Petroleum & Minerals, Dhahran 31261, Saudi Arabia
[3]Center for Research Excellence in Nanotechnology (CENT), King Fahd University of Petroleum & Minerals, Dhahran 31261, Saudi Arabia
[4]Center for Advanced Materials, Qatar University, Doha, Qatar
Correspondence to: M. A. Al-Harthi (E-mail: mamdouh@kfupm.edu.sa)

ABSTRACT: Polymer nanocomposites based on poly(vinyl alcohol) (PVA)/starch blend and graphene were prepared by solution mixing and casting. Glycerol was used as a plasticizer and added in the starch dispersion. The uniform dispersion of graphene in water was achieved by using an Ultrasonicator Probe. The composites were characterized by FTIR, tensile properties, X-ray diffraction (XRD), thermal analysis, and FE-SEM studies. FTIR studies indicated probable hydrogen bonding interaction between the oxygen containing groups on graphene surface and the –OH groups in PVA and starch. Mechanical properties results showed that the optimum loading of graphene was 0.5 wt % in the blend. XRD studies indicated uniform dispersion of graphene in PVA/starch matrix upto 0.5 wt % loadings and further increase caused agglomeration. Thermal studies showed that the thermal stability of PVA increased and the crystallinity decreased in the presence of starch and graphene. FE-SEM studies showed that incorporation of graphene increased the ductility of the composites. © 2015 Wiley Periodicals, Inc. J. Appl. Polym. Sci. **2015**, *132*, 41827.

KEYWORDS: biopolymers and renewable polymers; blends; composites; mechanical properties; properties and characterization

Received 28 June 2014; accepted 1 December 2014
DOI: 10.1002/app.41827

INTRODUCTION

The decline in the petroleum resources and an exponential increase in the usage of nonbiodegradable plastic films pose a great threat to the environment. Development of polymer blends and composites, which are amenable to biodegradation, has attracted wide attention in the recent years. Reinforcement of polymer matrices by nanofillers has been widely studied in the last two decades and lately graphene has emerged as a strong competitor for conventional nanofillers such as carbon nanotubes and nanoclays because of its outstanding mechanical and electrical properties, high aspect ratio, low density, and low cost.[1–4] Biodegradable polymer nanocomposites are usually weak in strength and susceptible to water and moisture. Providing adequate mechanical strength and structural integrity for their usage in packaging applications is a great challenge and is the motivation behind undertaking this research work.

Poly(vinyl alcohol), abbreviated as PVA, is a bio-degradable polymer whose properties are mainly governed by the degree of hydrolysis, molecular weight, and crystallinity.[5] PVA is widely used in the packaging and textile industries for its excellent properties such as film forming and biodegradability. Even though, PVA is considered to be a biodegradable material, the rate of its biodegradability is less than that of other biopolymers such as poly(hydroxyalkanoate) (PHA) or poly(lactic acid) (PLA).[6] Starch is a renewable, biocompatible, and biodegradable natural polymer, which is widely used to develop environmental friendly materials and can be easily blended with different polymers.[7,8] However, it lacks dimensional stability, physical strength, moisture resistance, thermal stability, and processability. PVA/starch blend is a widely studied biodegradable polymer blend because the rate of biodegradation of PVA can be improved with reduction in overall cost of the material.[9–11] Furthermore, the processability of this blend can be enhanced by using conventional plasticizers such as glycerol,[12] water, urea,[13] or citric acid[14] and the poor mechanical and thermal properties of the PVA/starch blend can be improved by irradiation,[15] chemical crosslinking,[16] physical crosslinking,[17] post curing,[18] modification of starch,[19] and incorporation of nanofillers.[20]

Table I. Formulation the PVA/Starch/Graphene Nanocomposites

Sample code	PVA (wt %)	Starch (wt %)	Graphene (wt %)	Water (mL)
PVA	100 (8.0)[a]	-	-	100
PSG (0.00)[a]	70 (5.6)[b]	30 (2.4)[c]	0.00 (0.00)[d]	50 + 50
PSG (0.25)[a]	70 (5.6)[b]	30 (2.4)[c]	0.25 (0.02)[d]	50 + 50 + 50
PSG (0.50)[a]	70 (5.6)[b]	30 (2.4)[c]	0.50 (0.04)[d]	50 + 50 + 50
PSG (0.75)[a]	70 (5.6)[b]	30 (2.4)[c]	0.75 (0.06)[d]	50 + 50 + 50
PSG (1.00)[a]	70 (5.6)[b]	30 (2.4)[c]	1.00 (0.08)[d]	50 + 50 + 50

Each formulation contains 3 mL of glycerol.
[a,b,c,d]Values in the parentheses stand for the weight in grams
[a]Values in the parentheses stand for the weight % of graphene in the composites.

PVA can be effectively reinforced by optimizing the process conditions in solution blending,[1,21] when the graphene nanosheets are fully exfoliated followed by hydrogen bonding between the oxygen-containing groups on graphene edges and the polymer matrix. The final properties of PVA-graphene nanocomposites can be manipulated by the surface modification of graphene.[22–24] A small amount of graphene addition into the PVA polymer could be effective to enhance the thermal stability, mechanical strength, biocompatibility, and conductivity. Rui *et al.* studied bio-nanocomposites of starch and graphene oxide with compatibility, resistance against moisture uptake, and increased thermal stability.[25] Polymer nanocomposites based on PVA/starch blend is relatively a new area of research and there are only a few reports based on montmorilonite nanoclay,[26] nano-SiO_2,[27] and zirconium phosphate[28] as the nanofillers. However, till date there is no report on the preparation and characterization of nanocomposites based on PVA/starch blend, using graphene as the nanofiller.

Blends of PVA/Starch have been studied in this laboratory[11,29,30] and it has been reported that optimum compatibility and improved mechanical properties can be obtained at PVA/starch blend ratio of 70/30 parts by weight, using glycerol as the processing aid. The present communication reports the results of our studies on the effect of graphene on the properties of the nanocomposites based on PVA/starch blend (PSG), with the objective to prepare an environment friendly polymer film, suitable for use in biomedical applications and packaging purposes.

EXPERIMENTAL

Materials

Corn starch was provided by ARASCO Corn Products, Dammam, Saudi Arabia. PVA (molecular weight, 27,000; degree of hydrolysis, 98.0–98.8 mol %) and glycerol and were procured from Sigma Aldrich Company. Graphene (Grafen®-iGP) of 96–99% purity (Oxygen content, ~ 1%, surface area, 13–15 m^2/g, and thickness 50–100 nm) was purchased from Grafen Chemical Industries, Turkey.

Preparation of Blends and Nanocomposites

The formulations are given in Table I. In order to ensure compatibility between the blend components,[11,29,30] PVA/starch blend ratio was kept constant at 70/30 in parts by weight. Solution of PVA was made with deionized water (50 mL) at 90°C under stirring. Dispersion of starch in water in the presence of glycerol (as a plasticizer for PVA/starch blend) was prepared separately. A dispersion of graphene in water was prepared by ultra sonication using the Ultrasonicator Probe (Ultrasonica Q 700) at an amplitude of 30% for 2 min. The graphene dispersion remained stable for more than 48 h without any settling of the graphene particles in water. Next the dispersions of starch and graphene were added to the PVA solution in water and the stirring was continued for three hours at 400 rpm. After degassing for 10 min, the mixture was poured onto a glass plate placed on a leveled flat surface and allowed to dry at 50°C for 24 h. The dried films of approximately 0.3 mm thickness were carefully peeled off from the glass plate and preserved in a desiccator to avoid any moisture uptake.

Characterizations of the Sample

The FTIR spectra were obtained by averaging 32 scans, at a resolution of 4 cm^{-1} from 500 to 4500 cm^{-1} by using a Thermo NICOLET 6700 FT-IR Spectrometer. Tensile tests were carried out according to ASTM D 882-12 at a speed of 50 mm/min by using a Universal Testing Machine (Lloyd 1 K LF PLUS-UTM). Tensile samples were prepared by cutting strip samples of 100 mm length and 15 mm width. At least five specimens of each composition were tested and the average values are presented. The results were reproducible with an accuracy of ±5%. Transmission electron microscope images were taken by JEOL, JEM 2011 (for high resolution TEM) and HITACHI H-7600. The X-ray diffraction (XRD) measurements were done by using a LABX XRD-6000, Shimadzu Diffractometer operating at 40 kV, 40 mA. X-rays of 1.541 A° wavelength generated by the Cu K_α source and the angle of diffraction (2θ) was varied from 2° to 40° in order to identify any changes in the crystal structure. Thermal degradation studies on samples weighing approximately 10 mg were made by using Perkin Elmer, Thermogravimetric Analyzer, Pyris-6 in nitrogen at a heating rate of 10°C per minute and in the temperature range of 25°C to 600°C. Differential scanning calorimetric (DSC) studies were made by using DSC-Q1000, Universal V4.2E TA Instruments in nitrogen at a heating rate of 10°C/min and in the temperature region of −70°C to 240°C. DSC calibration was done by measuring the temperature and the enthalpy of melting of indium. In the first scanning cycle, the sample was heated till 200°C to remove any thermal history and the crystallization curve was obtained while

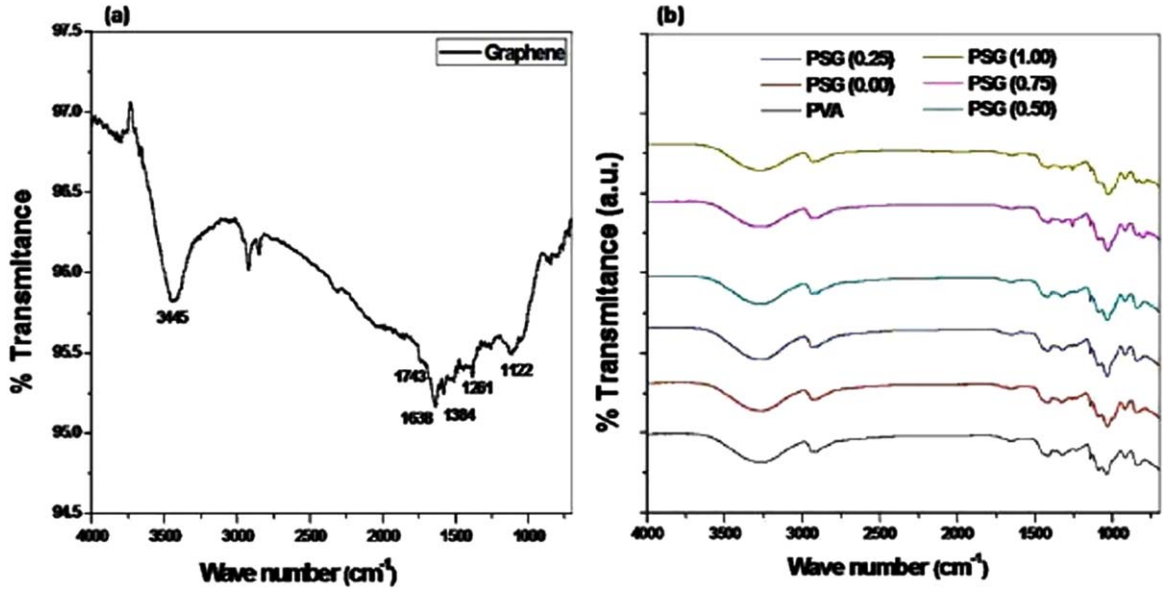

Figure 1. FTIR spectra: (a) graphene; and (b) PVA, PVA/starch blend and the nanocomposites at different graphene loadings. [Color figure can be viewed in the online issue, which is available at wileyonlinelibrary.com.]

cooling the sample. The glass transition temperature and melting enthalpy were recorded in the final heating scan. Cryo-fractured samples were gold coated and then scanning electron micrograph (SEM) images were taken by using LYRA3 TESCAN FE-SEM. The surface topography of PVA–starch blend and PVA–starch–graphene nanocomposite were analyzed using Agilent Atomic Force Microscope (Model No. 5500).

RESULTS AND DISCUSSION

FTIR Studies

FTIR results of graphene, PVA, and the nanocomposites are shown in Figure 1(a,b). Figure 1(a) shows the characteristic peaks of graphene, corresponding to –OH vibrations at 3200–3500 cm^{-1}, C=O stretching vibrations of carboxylic groups at 1743 cm^{-1}, skeletal vibrations from unoxidized graphitic domains at 1630 cm^{-1}, C-OH (hydroxyl) stretching vibration at 1384 cm^{-1}, C-O-C (epoxy) stretching vibration at 1261 cm^{-1} (fullerenol), and C-O stretching at 1122 cm^{-1}. Similar results on FTIR of graphene have been reported earlier.[31]

Figure 1(b) shows the FTIR spectra of PVA and the nanocomposites. The broad peak at 3200–3500 cm^{-1} is assigned to the stretching vibration of hydroxyl (–OH) groups and the absorption peak at 2926 cm^{-1} is because of the C–H stretching, while the hump at 1712 cm^{-1} corresponds to the C=O functional group and the peak at 1651 cm^{-1} is because of the bound water.[32] The peaks at 1422 and 846 cm^{-1} are because of the CH_2 group vibrations and the absorption at 1314 cm^{-1} is because of C-O-C group deformation and the peak at 1036 cm^{-1} is because of the stretching in aliphatic alcohols[33]. Since the characteristic peaks of glycerol and starch are similar to that of PVA,[34,35] the peak positions registered no change in the presence of glycerol and starch. The absorption band in the 3200–3500 cm^{-1} range of PVA/starch blend is attributed to both inter- and intra-molecular hydrogen bonded –OH groups in PVA and starch, which remained unaffected at low loading of graphene. However, higher loadings of graphene caused a decrease in intensity of this absorption band indicating occurrence of hydrogen bonding interactions between the OH-groups present in PVA/starch and oxygen containing groups in graphene, at the cost of inter- and intra-molecular hydrogen bonding in the PVA/starch blend.[26]

Mechanical Properties

Mechanical properties such as tensile strength, Young's modulus, and percentage elongation at break of PVA and the nanocomposites are shown in Table II. Incorporation of starch into the PVA matrix, as in formulation PSG(0.0), caused a fall in tensile properties of PVA. It was also found that the fall in properties could be arrested on incorporation of graphene in the PVA/starch system, as in PSG (0.25). Furthermore, as the loading of graphene was increased to 0.5 wt %, there was a further increase in tensile strength and modulus, though the ductility was still less than that of PVA. Further increase in graphene loading, as in formulations PSG(0.75) & PSG(1.00), caused a decrease in tensile properties presumably because of agglomeration of the nanoparticles.[36,37]

It is believed that the graphene nano-sheets disperse individually at low graphene loading of 0.25 wt %. However, at 0.5 wt %

Table II. Mechanical Properties of PVA/Starch/Graphene Systems

Sample	Tensile strength (MPa)	Young's modulus (MPa)	Elongation at fracture (%)
PVA	8.89	61.96	91.6
PSG (0.00)	6.67	24.23	27.5
PSG (0.25)	6.70	29.15	49.6
PSG (0.50)	10.04	53.33	57.2
PSG (0.75)	7.95	54.09	46.1
PSG (1.00)	7.75	46.27	38.9

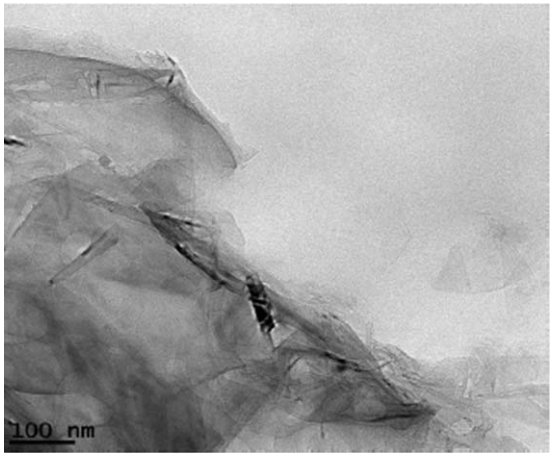

Figure 2. TEM image of the nanocomposite, PSG(0.50).

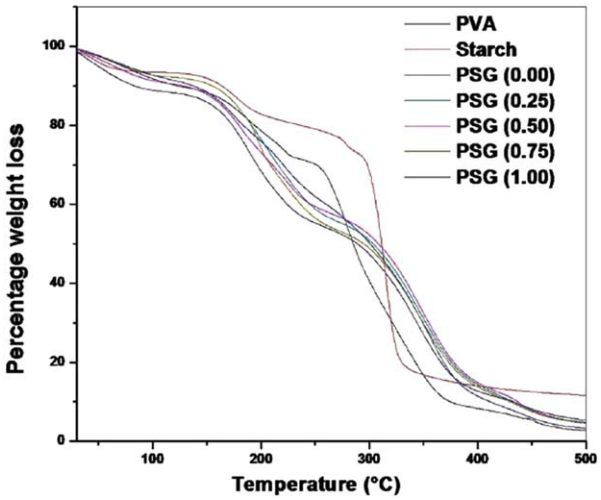

Figure 4. TGA plots of PVA, PVA/starch blend and the nanocomposites. [Color figure can be viewed in the online issue, which is available at wileyonlinelibrary.com.]

loading of the nanofiller, the edges of the sheets might just join together side by side. This may lead to efficient load transfer between the matrix and the filler, causing enhancement in mechanical properties. TEM image of PSG(0.5) nanocomposite is shown in Figure 2. The graphene layers in polymer matrices appeared flat with folding and wrinkles on the surface and edges,[38] which contribute to the enhanced interaction with the polymer chains via physical interlocking mechanism. As the graphene loading was increased further, the individual sheets tend to restack together to form agglomerates. This sort of arrangement weakens the interface between graphene and the polymer components, causing a drop in the properties.[39]

XRD Studies

Figure 3(a) shows the XRD diagrams of PVA, starch, and graphene. The major characteristic peak of PVA appeared at 19.9° 2θ and the minor peaks appeared at 11.0° and 22.5° 2θ. The less intense peaks for starch appeared in 15.2°, 17.4°, 19.0°, and 23.1° 2θ, which correspond to the XRD pattern of a mixture of A-type and Vh-type crystal structure present in starch.[11,29,30] The XRD peak of graphene nanosheets appeared at 26.6° 2θ, implying that the *d*-spacing is similar to the (002) plane of pristine graphite.[40]

In the case of nanocomposites, the diffraction patterns are dependent on the graphene loadings [Figure 3(b)]. At low loadings of 0.25 and 0.5 wt %, the diffraction patterns are similar to that of PVA. The absence of the characteristic peak of graphene shows that the nanosheets were exfoliated and individually dispersed in the polymer matrix. As the graphene loading was increased to 0.75 and 1.00 wt %, the characteristic peak of graphene reappeared, but with less intensity. This is indicative of

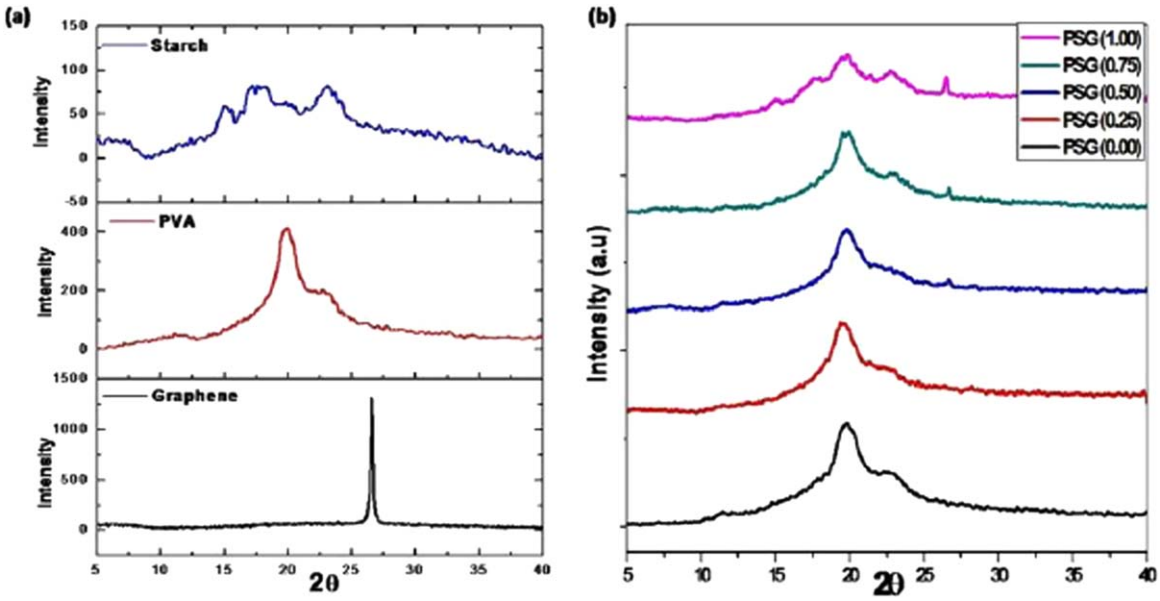

Figure 3. XRD plots: (a) PVA, starch, and graphene; (b) PVA/starch blend and the nanocomposite. [Color figure can be viewed in the online issue, which is available at wileyonlinelibrary.com.]

Table III. The TGA and DSC Results for PVA/Starch/Graphene Nanocomposites

Sample	Degradation onset temperature (°C)	Degradation temperature (T_d) (°C)	Residue at 500°C (wt %)	T_g (°C)	ΔH_m (W/g)	T_m (°C)	T_c (°C)
PVA	191	329	2.73	38.5	44.9	207.6	182.6
PSG (0.00)	151	356	3.28	69.6	33.8	227.7	203.1
PSG (0.25)	150	348	4.55	42.4	28.2	215.3	191.4
PSG (0.50)	143	347	4.75	49.4	27.4	218.6	194.7
PSG (0.75)	146	346	4.96	43.3	27.8	215.6	189.9
PSG (1.00)	147	345	5.35	47.7	27.6	219.9	193.6

the agglomeration of graphene nanosheets in the polymer matrix, which leads to weakening of the interfacial adhesion between the nanosheets and the polymer components. This causes a fall in tensile properties of the composites, as discussed earlier.

TGA Studies

Figure 4 shows the TGA plots of PVA, PVA/starch blend, and the graphene nanocomposites. It is evident the degradation of PVA occurred primarily in two stages: the first one between 150°C and 250°C and the second one between 250°C and 400°C. The onset temperature of degradation reaction of PVA was significantly reduced by 40°C by the blending process with starch. The addition of graphene into the blends again showed a marginal decreasing trend. The degradation in the case of blends and nanocomposites started at lower temperature implies the degradation of the interface of PVA/starch or PVA/Graphene. Incorporation of starch caused some degree of overlapping between the two main degradation steps, causing a shift of the second degradation temperature to a higher temperature (i.e., from 329°C to 356°C).[41] This is because of the compatibility between PVA and starch, wherein thermally resistive cyclic hemiacetal in starch structure imparts thermal stability to the PVA/starch blends.[42] Incorporation of graphene caused a slight drop in the major degradation temperature (i.e., from 356°C to 348°C), which is independent of the nanofiller loading. Expectedly, the percent residue at 500°C increased with an increase in the graphene loading (Table III). Interestingly, the overlapping of the two degradation temperatures was also observed in the case of the nanocomposites at graphene loadings of 0.25 and 0.5 wt %. As the nanofiller concentration was increased to 0.75 and 1.00 wt %, the two degradation temperature zones appeared prominently. This implies an increase in the heterogeneity of the polymer components at higher graphene loading, presumably because of aggregation of the nanosheets as discussed earlier.[29,30,43]

DSC Results

Figure 5(a,b) is the thermograms showing the heating and cooling curves and the results are summarized in Table III. It is found that both T_g and T_m of PVA increased in the presence of starch, presumably because of stiffening effect on hydrogen bonding interaction with starch.[17,41] Incorporation of graphene, however, caused lowering of both T_g and T_m, which is believed to be because of a weakening of the PVA–starch bonding in the presence of the nanofiller.[38] Higher T_g in the case of 0.5 wt % loading of graphene indicates higher extent of bonding between the nano-filler and the polymer matrices with optimum dispersion. The heat of melting (ΔH_m) PVA was decreased

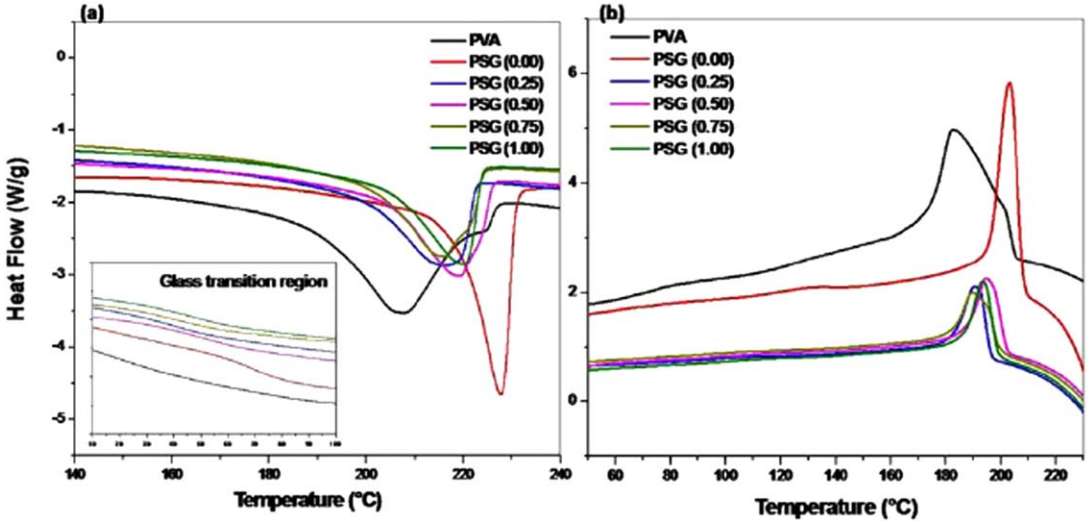

Figure 5. DSC thermograms: (a) heating; and (b) cooling curves of PVA, PVA/starch blend, and the nanocomposites. [Color figure can be viewed in the online issue, which is available at wileyonlinelibrary.com.]

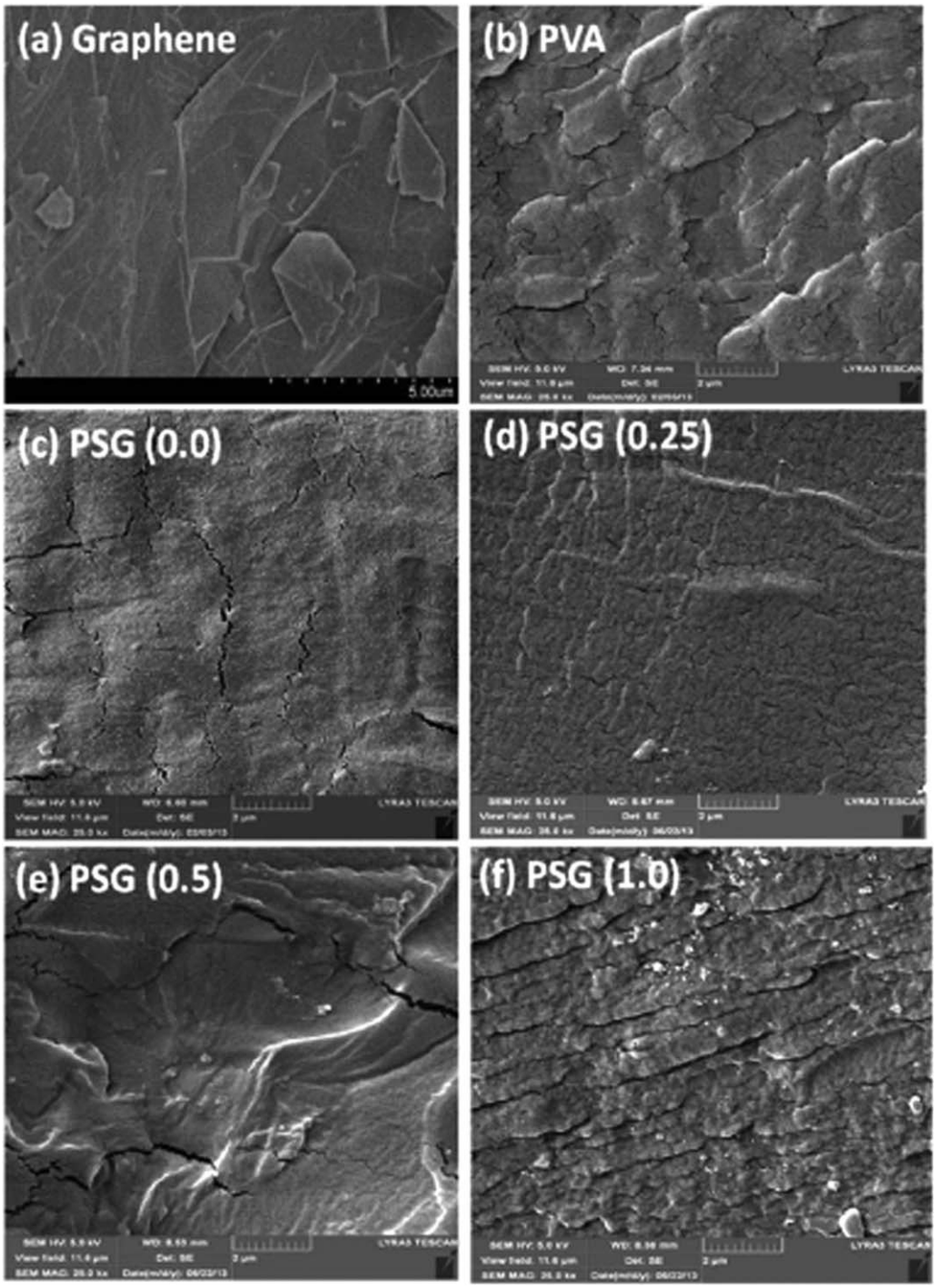

Figure 6. FE-SEM images: (a) Graphene, (b) PVA, (c) PSG(0.0), (d) nanocomposite at 0.25 wt % graphene loading, (e) nanocomposite at 0.50 wt % graphene loading, and (f) nanocomposite at 1.0 wt % graphene loading.

significantly, which indicates the decrease in the percentage crystallinity of PVA in the blend/composites systems. However, incorporation of graphene did not cause further significant changes in crystallinity of PVA.

FE-SEM and AFM Studies

The FE-SEM images of graphene, PVA, PVA/starch blend, and the nanocomposites are shown in Figure 6(a–f). Figure 6(a) shows that the graphene flake with typical wrinkled surface morphology and composed of several layers of graphene and the edges of each layer were clearly visible with different contrast on the image. Figure 6(b) shows the brittleness of PVA, while Figure 6(c) shows an increase in brittleness in the case of PVA/starch blend, as is evident from the increased number of surface cracks. The incorporation of graphene into the PVA/starch matrices improved the

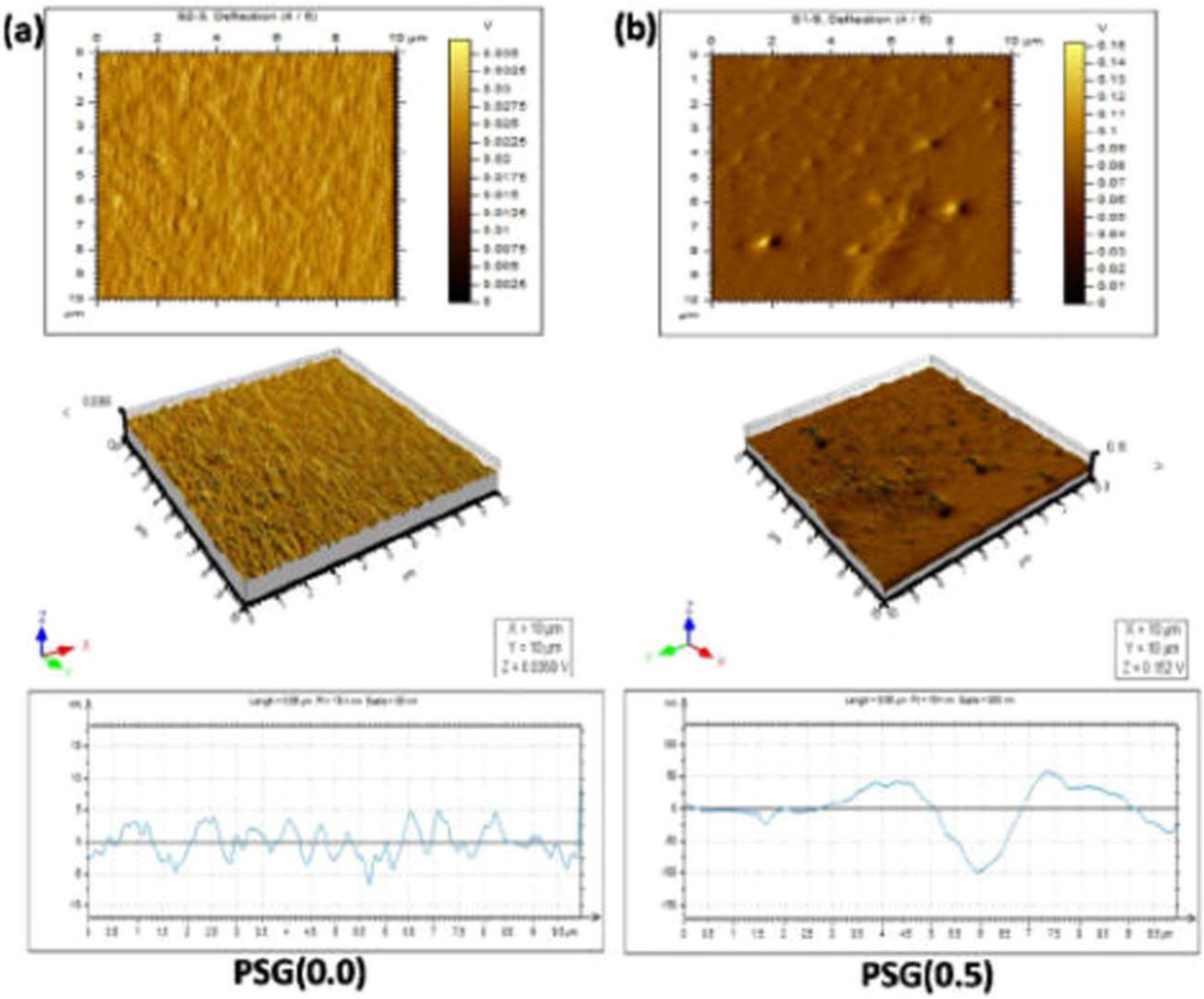

Figure 7. AFM images of (a) PSG(0.0) and (b) PSG(0.5) nanocomposite. [Color figure can be viewed in the online issue, which is available at wileyonlinelibrary.com.]

ductility with surface morphology change, which is corroborated with the increased elongation at break reported previously in the mechanical property analysis [Figure 6(d–f)]. The individual graphene sheets are not visible in the images of the composites, since the nanosheets are encapsulated by the polymer components.[44]

The surface characteristics of PVA–starch blends have been completely changed after the incorporation of graphene [Figure 7(a,b)]. The graphene nanosheets of irregular size and shapes were randomly distributed and embedded in the PVA–starch blend matrix. The polymer chains of PVA and starch would easily coat the nanosheets because of the hydrogen bonds between the hydrophilic polymers (PVA and starch) chains and basal planes of graphene nanosheets. The polymer coating of the graphene in the molecular level would enhance the interlayer interaction and caused efficient transfer of applied force between polymer and nanosheets. On the other hand, the polymer chains were able to bridge the adjacent nanoparticle on the same plane and effectively resisted the deformation between nanosheets of same plane during tensile loading. This is in correlation with the improved tensile strength of PVA/starch/graphene nanocomposite with optimum filler loading. In conclusion, both the polymer coating and graphene nanosheet bridging enhanced effective load transfer between the filler particles and hence overall improvement in mechanical properties.

CONCLUSIONS

Graphene was well dispersed in PVA/starch matrix via solution blending to prepare polymer nanocomposites films. The FTIR results indicated the existence of hydrogen bonding interaction between graphene and the PVA/starch matrix. The maximum tensile strength was obtained at a graphene loading of 0.5 wt %. Results of XRD studies show that the graphene nanoplatelets were dispersed uniformly in the polymer matrix. The thermal analyses show that there is an increase in thermal stability and a decrease in crystallinity of PVA because of the presence of starch and graphene. Furthermore, the surface morphology of PVA changed from brittle to ductile nature on blending of starch and incorporation of graphene.

ACKNOWLEDGMENTS

Thanks are due to the Deanship of Scientific Research for financial assistance through project number DSR IN121016. Thanks are also due to Center of Research Excellence in Nanotechnology (CENT), KFUPM for providing facilities for sample characterization.

REFERENCES

1. Compton, O. C.; Nguyen, S. B. T. *Small* **2010**, *6*, 711.
2. Michele, T. B.; Yurii, K. *Adv. Mater.* **2010**, *22*, 1672.
3. Sheshmani, S.; Ashori, A.; Arab, F. M. *Int. J. Biol. Macrmol.* **2013**, *58*, 1.
4. Sheshmani, S.; Amini, R. *Carbohydr. Polym.* **2013**, *95*, 348.
5. Peppas, N. A.; Merrill, E. W. *J. Biomed. Mater. Res.* **1977**, *11*, 423.
6. Chiellini, E.; Corti, A.; Solaro, R. *Polm. Degrad. Stab.* **1999**, *64*, 305.
7. Fang, Y.; Kalappa, P.; Jeremie, S.; Marie-France, L.; Patricia, K. *Carbohydr. Polym.* **2013**, *91*, 253.
8. Ashori, A. *Polym. Eng. Sci.* **2013**, doi: 10.1002/pen.23774.
9. Xiaozhi, T.; Sajid, A. *Carbohydr. Polym.* **2011**, *85*, 7.
10. Wan-Lan, C.; Jing-Dong, C.; Chien-Chung, C. *J. Polym. Environ.* **2012**, *20*, 550.
11. Sreekumar, P. A.; Al-Harthi, M. A.; De, S. K. *Polym. Eng. Sci.* **2012**, *52*, 2167.
12. Liu, Z. Q.; Feng, Y.; Yi, X. S. *J. Appl. Polym. Sci.* **1999**, *74*, 2667.
13. Ma, X.; Yu, J.; Jin, F. *Polym. Int.* **2004**, *53*, 1780.
14. Zou, G. X.; Jin, P. Q.; Xin, L. Z. *J. Elastom. Plast.* **2008**, *40*, 303.
15. Zhai, M.; Yoshii, F.; Kume, T. *Carbohydr. Polym.* **2003**, *52*, 311.
16. Yoon, S. D.; Chough, S. H.; Park, H. R. *J. Appl. Polym. Sci.* **2007**, *106*, 2485.
17. El-Refaie, K.; Elbadawy, A. K.; Mohamed, S. M. E.; El-Meligy, M. A. *Arab. J. Chem.* **2013**, doi:10.1016/j.arabjc.2013.05.026.
18. Ziqin, L.; Yan, D.; Haitao, M.; Man, J.; Jin, T.; Jiang, Z. *Carbohydr. Polym.* **2012**, *89*, 473.
19. Lee, W. J.; Youn, Y. N.; Yun, Y. H.; Yoon, S. D. *J. Polym. Environ.* **2007**, *15*, 35.
20. Soon-Do, Y.; Mi-Hwa, P.; Hun-Soo, B. *Carbohydr. Polym.* **2012**, *87*, 676.
21. Lee, S.; Jin-Yong, H.; Jyongsik, J. *Polym. Int.* **2013**, *62*, 901.
22. Liang, J. J.; Huang, Y.; Zhang, L.; Wang, Y.; Ma, Y. F.; Guo, T. Y.; Chen, Y. S. *Adv. Funct. Mater.* **2009**, *19*, 1.
23. Salavagione, H. J.; Gomez, M. A.; Martinez, G. *Macromolecules* **2009**, *42*, 6331.
24. Zhou, T.; Chen, F.; Tang, C.; Bai, H.; Zhang, Q.; Deng, H.; Fu, Q. *Compos. Sci. Technol.* **2011**, *71*, 1266.
25. Rui, L.; Changhua, L.; Jun, M. *Carbohydr. Polym.* **2011**, *84*, 631.
26. Dean, K. M.; Do, M. D.; Petinakis, E.; Yu, L. *Compos. Sci. Technol.* **2008**, *68*, 1453.
27. Tang, S.; Zou, P.; Xiong, H.; Tang, H. *Carbohydr. Polym.* **2008**, *72*, 521.
28. Yang, Y.; Liu, C.; Chang, P. R.; Chen, Y.; Anderson, D. P.; Stumborg, M. *J. Appl. Polym. Sci.* **2010**, *115*, 1089.
29. Sreekumar, P. A.; Al-Harthi, M. A.; De, S. K. *J. Compos. Mater.* **2012**, *46*, 3181.
30. Sreekumar, P. A.; Al-Harthi, M. A.; De, S. K. *J. Appl. Polym. Sci.* **2012**, *123*, 135.
31. Qin, L.; Beidou, G.; Jiaguo, Y.; Jingrun, R.; Baohong, Z.; Huijuan, Y.; Jian, R. G. *J. Am. Chem. Soc.* **2011**, *133*, 10878.
32. Wolkers, W. F.; Oliver, A. E.; Tablin, F.; Crowe, J. H. *Carbohydr. Res.* **2004**, *339*, 1077.
33. Tahira, P.; Sara, A. A.; Carl, D. S.; Sakhawat, S. S.; Saad, A. K. *Langmuir* **2012**, *28*, 5834.
34. Lima, E.; Raphael, E.; Sentanin, F.; Rodrigues, L. C.; Ferreira, R. A. S.; Carlos, L. D.; Silva, AP; M. M. *Mater. Sci. Eng. B* **2012**, *177*, 488.
35. Guan, Y.; Qian, L.; Xiao, H.; Zheng, A. *Cellulose* **2008**, *15*, 609.
36. Arun, K.; Xu, L. R. *J. Nat. Mater.* **2012**, doi:10.1155/2012/483093.
37. Chaharmahali, M.; Yahya, H.; Ghanbar, E.; Alireza, A.; Ismail, G. *Polym. Bull.* **2013**, doi:10.1007/s00289-013-1064-3.
38. Rui, S.; Jingliang, B.; Zizheng, Z.; Aichen, Z.; Dafu, C.; Xinhua, Z.; Liqun, Z.; Wei, T. *Carbohydr. Polym.* **2008**, *74*, 763.
39. Jeffrey, R. P.; Daniel, R. D.; Christopher, W. B.; Rodney, S. R. *Polymer* **2011**, *52*, 5.
40. Li, W.; Liang, C.; Zhou, W.; Qiu, J.; Zhou, Z.; Sun, G.; Xin, Q. *J. Phys. Chem. B* **2003**, *107*, 6292.
41. Xuegang, L.; Jiwei, L.; Xiaoyan, L. *Carbohydr. Polym.* **2012**, *90*, 1595.
42. Liu, X. X.; Yu, L.; Liu, H. S.; Chen, L.; Li, L. *Polym. Degrad. Stab.* **2008**, *93*, 260.
43. Mallick, A.; Tripathy, D. K.; De, S. K. *Rubber. Chem. Technol.* **1994**, *67*, 845.
44. Shanshan, T.; Qingwen, L.; Yanchun, L.; Weihong, Z.; Qiong, J.; Taicheng, D. *J. Chromatogr. A* **2012**, *1253*, 22.